PAPER

Breath biomarkers of total body irradiation in non-human primates

Journal of Breath Research

PAPER

Breath biomarkers of total body irradiation in non-human primates

Michael Phillips[1,2,*], Felix Grun[3] and Peter Schmitt[4]

[1] Menssana Research Inc, I Horizon Rd, Suite 1415, Fort Lee, NJ, 07024-6510, United States of America
[2] Department of Medicine, New York Medical College, Valhalla, NY, United States of America
[3] Mass Spectrometry Facility, University of California Irvine, Irvine, CA, 92697-2025, United States of America
[4] Schmitt & Associates, 211 Warren St, Newark, NJ, 07103, United States of America
[*] Author to whom any correspondence should be addressed.

E-mail: mphillips@menssanaresearch.com

RECEIVED
15 July 2021

REVISED
10 November 2021

ACCEPTED FOR PUBLICATION
15 November 2021

PUBLISHED
11 January 2022

Keywords: radiation biodosimetry, total body irradiation, non-human primates, breath, biomarkers, volatile organic compounds, oxidative stress

Abstract

Background. Radiation exposure causes oxidative stress, eliciting production of metabolites that are exhaled in the breath as volatile organic compounds (VOCs). We evaluated breath VOCs as potential biomarkers for use in radiation biodosimetry. *Methods.* Five anesthetized non-human primates receive total body irradiation (TBI) of three daily fractions of 120 cGy per day for three days, resulting in a cumulative dose of 10.8 Gy. Breath samples were collected prior to irradiation and after each radiation fraction, and analyzed with gas chromatography mass spectrometry. *Results.* TBI elicited a prompt and statistically significant increase in the abundance of several hundred VOCs in the breath, including some that were increased more than five-fold, with100% sensitivity and 100% specificity for radiation exposure. The most significant breath VOC biomarkers of radiation mainly comprised straight-chain n-alkanes (e.g. hexane), as well as methylated alkanes (e.g. 3-methyl-pentane) and alkane derivatives (e.g. 2-butyl-1-octanol), consistent with metabolic products of oxidative stress. An unidentified breath VOC biomarker increased more than ten-fold following TBI, and rose linearly with the total cumulative dose of radiation ($R^2 = 0.92$). *Conclusions.* TBI of non-human primates elicited increased production of breath VOCs consistent with increased oxidative stress. These findings provide a rational basis for further evaluation of breath VOC biomarkers in human radiation biodosimetry.

1. Introduction

Wilhelm Conrad Roentgen discovered X-radiation in 1895, and within months, other researchers reported that these new rays could cause harmful effects such as skin burns. It is now known that exposure to ionizing radiation, whether medical, occupational or accidental, can have serious biological consequences including increased risk of cancer and death [1]. In order to help minimize these consequences, researchers have sought to develop biodosimeters that can estimate the biological effects of ionizing radiation. Several different technical approaches have been proposed including detection of electron paramagnetic resonance in tissues [2], induced chromosomal abnormalities [3], altered gene expression [4] and modified circulating proteins [5].

Breath testing for oxidative stress products potentially provides a non-invasive alternative tool for radiation biodosimetry. Radiation energy ionizes water by ejecting orbital electrons and generating an ion radical:

$$H_2O + \text{ radiation } \rightarrow H_2O^{+*} + e^-.$$

The ion radical oxidizes polyunsaturated fatty acids (e.g. arachidonic acid) in cell membranes and elicits a cascade of downstream oxidative events. The metabolic products of the cascade include n-alkanes (e.g. pentane, hexane) and alkane derivatives that are exhaled in the breath as volatile organic compounds (VOCs) [6, 7].

An early case study reported that radiation-induced oxidative stress was associated with increased of ethane in exhaled breath [8]. Irradiation of animal and plant tissues in foodstuffs also elicits production of several different VOCs, including alkanes and

alkenes consistent with oxidative stress products, as well as benzene derivatives and aldehydes [9–11].

We have previously reported breath VOC biomarkers of radiation in humans and in Göttingen minipigs [12, 13], and we report here a study of breath VOC production following whole-body gamma irradiation of non-human primates. Results were consistent with previous findings and we also identified new candidate biomarkers that could potentially be employed for radiation biodosimetry.

2. Methods

2.1. Animals

The experimental cohort comprised five healthy female Rhesus monkeys (Macaca mulatta) weighing 5–6.7 kg and aged 6–7 years at the start of irradiation. The animal studies were performed at CiTox Lab North America (Laval, Quebec, Canada H7V 4B3) and approved by the Institutional Animal Care and Use Committee.

2.2. Radiation procedure

Animals were exposed to three daily fractions of 120 cGy for three days, for a cumulative dose of 10.8 Gy. This dosage regimen was adopted because it is similar to the dosage plan widely employed in treatment of humans with thoracic tumors. Ten samples were collected from each animal: Sample #0 two weeks prior to radiation (baseline), followed by samples #1 to #3 on day zero, #4 to #6 on day two, and #7-#9 on day three. All samples including sample #0 prior to radiation were collected in the same fashion as described below, employing a helmet and sedation. Prior to irradiation, dosage was calibrated using an acrylic phantom placed in the same experimental set up used for animal irradiation in which each animal was placed in a restraining chair in a symmetrical position. Uniform total body dose radiation (divided into equal anterior and posterior exposures) was administered from a Co^{60} source (Theratron 1000) at a dose rate of approximately 50 cGy min^{-1}. Irradiation dosage was monitored with two dosimeters (Landauer, Inc. Model nanoDot) and a Farmer ionization chamber connected to an electrometer. Animals were treated with analgesics (buprenorphine 0.01 mg kg^{-1} twice daily) and antiemetics (ondansetron 1 mg kg^{-1}) IM) before and after radiation. All animals were euthanized at the end of the experiment.

2.3. Collection of breath samples

Breath samples were collected from a clear plastic helmet that enclosed the animal's head and neck. Animals breathed room air at all times. The helmet was open at neck level and there was no restriction of inflow of room air. Mixed expiratory breath was drawn from the apex of the helmet above the animal's head. Using a calibrated sampling pump, duplicate samples of 1.0 l breath were withdrawn from the helmet through sorbent traps containing graphitized carbon black at a rate of 0.5 l min^{-1} for 2.0 min. Following collection of a sample, each sorbent trap was immediately sealed in a hermetic storage container (Carbotrap® in stainless steel TD tube and TDS [3] Storage Container, Supelco, Inc. Bellefonte, PA 16823).

2.4. Analysis of breath VOCs

Breath VOC samples were analyzed in the Mass Spectrometry Facility of the University of California, Irvine, CA. The sorbent traps were analyzed by automated thermal desorption (ATD) on a gas chromatography mass spectrometry/flame ionization detection (ATD GC-MS/FID) system. The instrument platform consisted of a TD-100xr autosampler (Markes International, Inc., Sacramento, CA), Agilent 8890 GC with FID and 5977B MSD (Agilent Technologies, Santa Clara, CA).

Instrument parameters were as follows: Thermal desorption tubes were desorbed at 250 °C for 1 min and volatiles recondensed onto the autosampler trap held at 30 °C. For transfer to the GC column, the trap was rapidly heated to 300 °C at 40 °C s^{-1} with a split carrier flow of 20 ml min^{-1}. The GC column was an Agilent HP-5MS UI column (30 m × 0.25 mm, 0.25 μm; Agilent Technologies Inc., Santa Clara, CA) with the following GC gradient parameters: initial isothermal hold at 35 °C for 5 mins, 20 °C min^{-1}–300 °C over 13 mins, final 2 min hold at 300 °C; constant carrier flow at 3 ml min^{-1}. The GC flow was split post-column to the MS and FID detectors. The MS detector collected data in EI mode for the m/z range of 30–650 at 2.4 scans/sec.

Data was analyzed with Mass Hunter software (Agilent Technologies, Inc., Santa Clara, CA). Component spectra were searched against the NIST 2017 MS spectral database library for analyte identification.

2.5. Analysis of data for discovery of candidate breath biomarkers of radiation

Animals acted as their own controls prior to irradiation. Prior studies have shown that repetitive samples collected under the same conditions are very stable, and that their pre-irradiation breath VOCs chromatograms were consistently similar to the typical Day zero chromatogram shown in figure 1. We analyzed the data with two different tools in order to identify candidate breath VOC biomarkers of radiation: Multiple Monte Carlo simulations that compared the area under curve (AUC) values of breath VOCs from scans of the TIC traces, and MetaboAnalyst partial least squares discriminant analysis (PLSDA) and sparse-PLSDA for significant feature

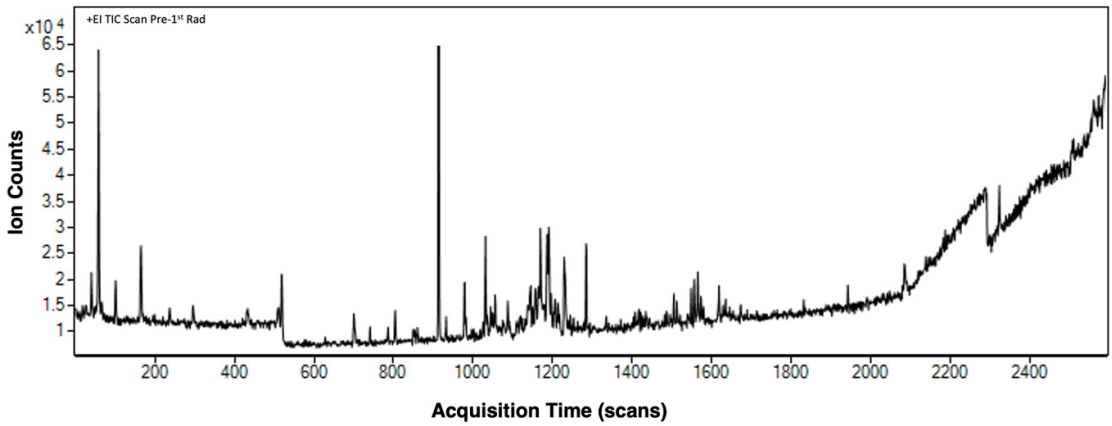

Figure 1. A typical breath VOC chromatogram prior to irradiation. This figure displays a typical GC MS chromatogram of breath VOCs collected from an animal on Day zero prior to irradiation. The horizontal axis displays the chromatographic retention time (min) and corresponding scan number. The vertical axis displays the intensity of the total ion current (TIC) of VOCs in breath at each time point. MassHunter peak detection algorithms resolved 133 peak features (average peak width 2.5 s or 6 scans/peak); Monte Carlo simulations used input data from of TIC intensities at 2600 scan points over 18 min chromatograms. These chromatographic peaks were consistently present in all animals prior to radiation. As the TIC values indicate, the abundance of breath VOCs was increased by at least an order of magnitude follow radiation.

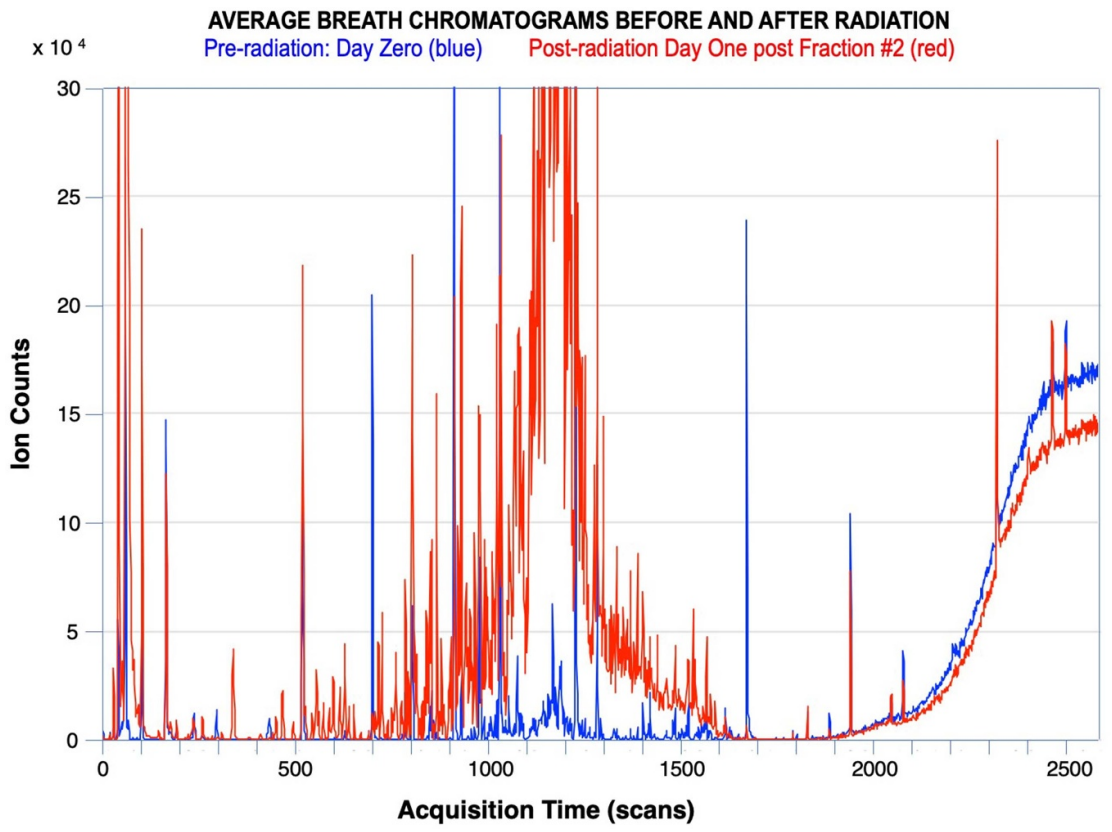

Figure 2. Comparison of pooled breath VOC chromatograms before and after irradiation. Averaged TIC traces are shown of pooled duplicate breath VOC chromatograms from the five animals at two points in time: Pre-irradiation (blue) on Day Zero and post-irradiation (red) collected following the second fraction of radiation on Day 1. The post-irradiation chromatograms displayed a broad global increase in breath VOCs compared to pre-irradiation levels.

selection and classification of peak 'rt_m/z' features curated from the datasets.

2.6. Multiple Monte Carlo simulations

The method has been described [14–16]. In summary, breath VOC chromatograms were assigned to two groups: pre-radiation (controls), and post-radiation. Apparent biomarkers of radiation exposure with greater than random accuracy were identified by their C-statistic values (i.e. AUC of the receiver operating characteristic) [17].

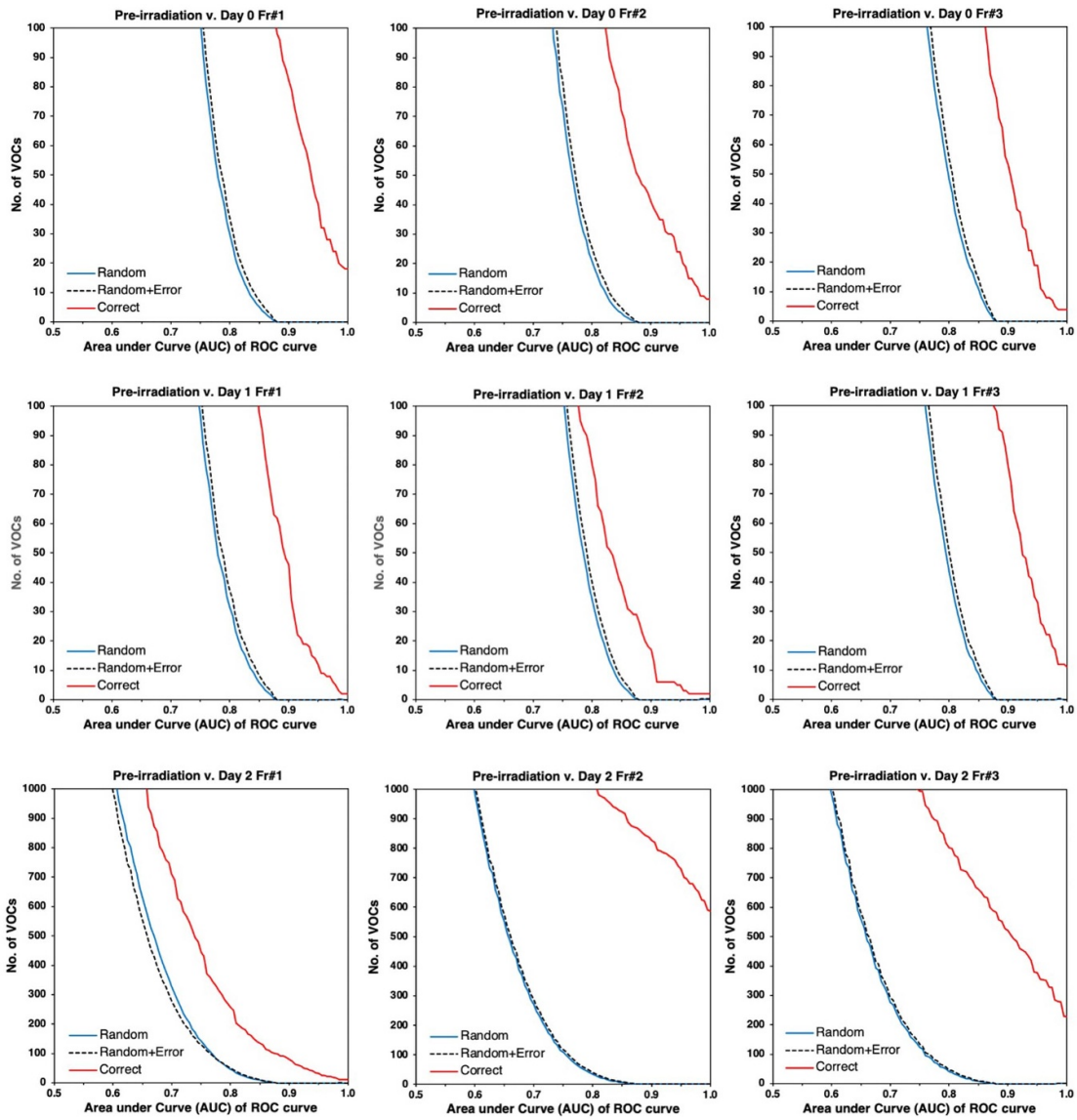

Figure 3. Monte Carlo simulations. The upper, middle and lower rows display the Monte Carlo simulations following exposure to radiation on Days zero, one and two respectively. Each panel displays the number of VOCs versus the C-statistic i.e. the area under curve (AUC) of the receiver operating characteristic (ROC) curve for the correct and random assignments of data. Each row displays results following radiation fractions 1, 2, and 3 respectively. The separation between the random assignment curve (blue) and the correct assignment curve (red) indicates the number of breath VOCs biomarkers with a diagnostic accuracy greater than expected by chance alone. As an example, the top left panel (Day zero fraction 1) displays 80–100 VOC scans in the correct assignment curve with diagnostic accuracy greater than expected by chance alone, so they were statistically significant biomarkers of radiation exposure. Note: the average number of scans for a distinct peak feature is about 6 or 2.5 s peak width. 20 VOC scans in the correct assignment curve, had a C-statistic equal to 1 i.e. they were 100% sensitive and 100% specific for detection of radiation exposure.

MetaboAnalyst [18] provides a set of online tools tailored for metabolomic data analysis and interpretation to aid in biomarker discovery and classification. MassHunter Quantitation software was used to batch process sample sets and extract peak features. Missing values were resolved by addition of a uniform small positive value (half minimum value) to all peak area data to improve downstream statistical calculations. Component peak areas were also normalized to an adjusted TIC peak area for each run. The adjusted TIC was calculated by subtracting the 5 most prominent peaks from the total peak area to minimize skewing of the data by a set of variable prominent features. Component data (component # (ID), retention time (RT) and normalized peak area (Int) were exported as .CSV input files for Metaboanalyst statistical analyses. Principal component analysis, orthogonal (o-PLSDA) and sparse partial least squares discriminant analysis (s-PLSDA) for binary and group comparisons respectively, and pattern hunter analysis for time trends were performed to identify candidate biomarker features of radiation exposure.

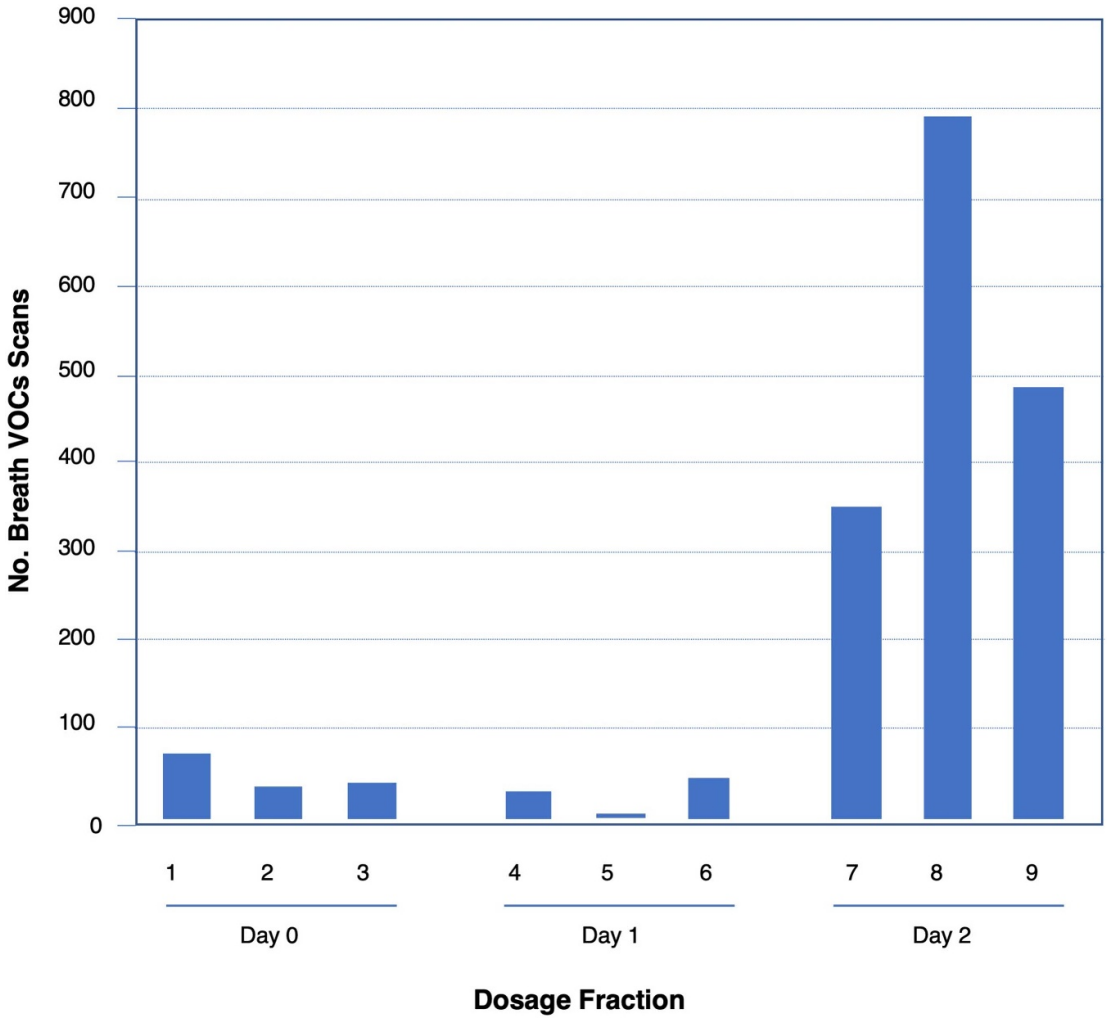

Figure 4. Variation in number of biomarker VOCs with cumulative dose of radiation. The figure displays the number of significantly increased breath VOC scans following radiation fractions 1, 2, and 3 on days zero, one and two respectively compared to the pre-radiation baseline control. The number of significant VOCs scans at each time point was derived from the Monte Carlo simulations shown in figure 3.

3. Results

A typical pre-irradiation breath VOC chromatogram collected from an animal on Day zero prior to irradiation is shown in figure 1.

3.1. Average breath chromatograms before and after radiation

The duplicate breath chromatograms of the five animals were pooled at each time point, and the average breath VOC abundances were determined.

Figure 2 displays the average of the pooled duplicate breath VOC chromatograms from the five animals at two points in time: Pre-irradiation on Day Zero and post-irradiation following the second fraction of radiation on Day 1. Total body irradiation (TBI) elicited more than a five-fold increase in the abundance of several VOCs.

3.2. Monte Carlo simulations

Figure 3 displays Monte Carlo simulations following radiation fractions 1, 2, and 3 on days zero, one and two respectively. At every time point in the study, the separation between the curves of random assignment and the correct assignment indicated that several breath VOCs biomarkers exhibited diagnostic accuracy greater than expected by chance alone, including a subset of VOCs with a C-statistic value of 1.0 i.e. these biomarkers were 100% sensitive and 100% specific for radiation exposure.

3.3. Variation in number of biomarker VOCs with cumulative dose of radiation

Figure 4 displays the number of significantly increased breath VOC scans in the chromatograms following radiation fractions 1, 2, and 3 on days zero, one and two respectively, as shown by the

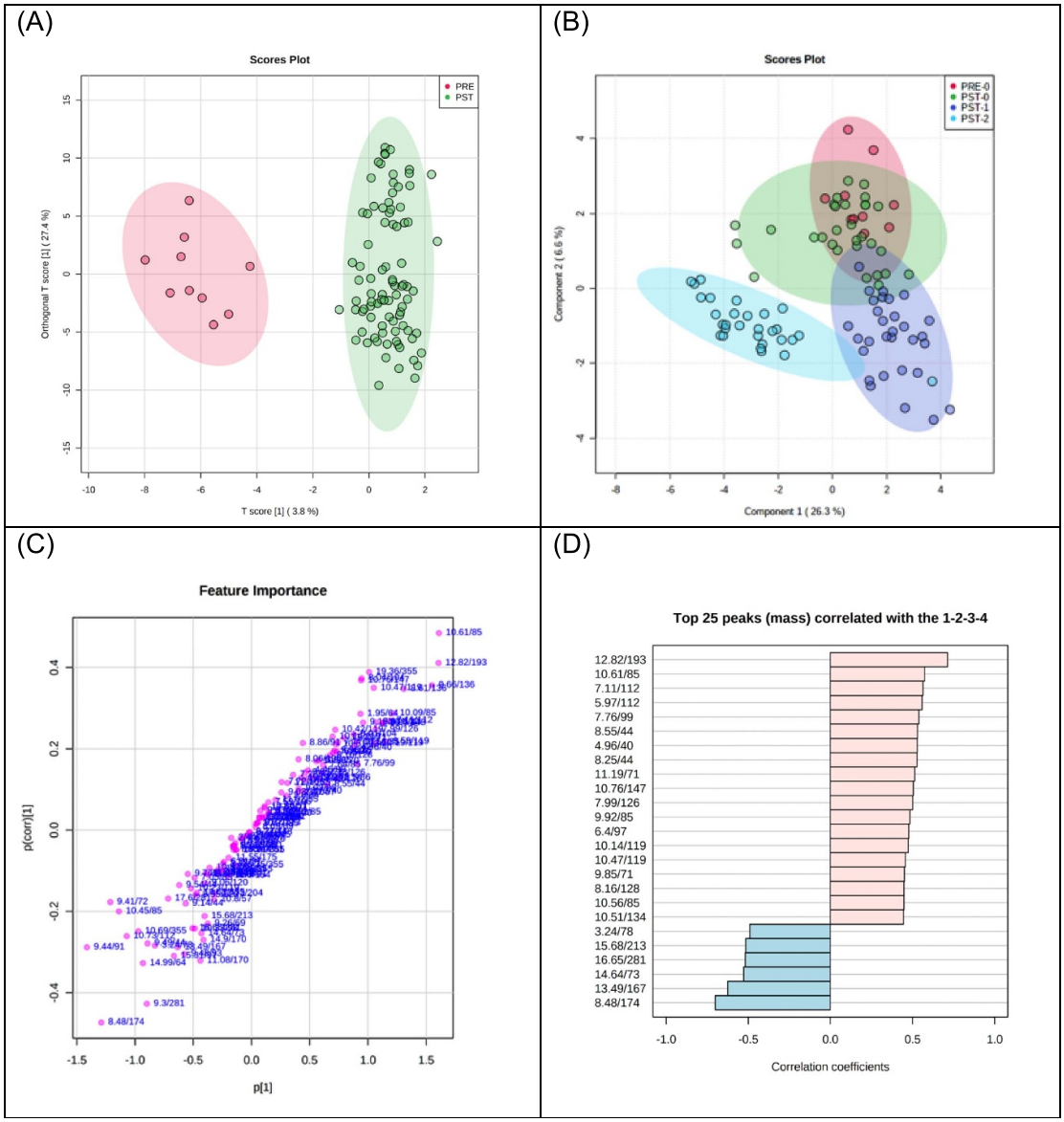

Figure 5. Partial Least Squares Discriminant Analyses and Pattern Hunter. (A) Scores plot of the o-PLSDA model comparing pre- versus all post-radiation samples that maximizes the separation between the groups. The post-irradiation samples were well classified and clustered distinctly from the pre-irradiation samples suggesting component features can discriminate between group treatment. (B) Scores plot of the S-PLSDA model for a multi-group comparison of pre-radiation (PRE-0), post Day Zero (PST-0), post Day One (PST-1), and post Day Two (PST-2) groups. Discrimination between groups increased with time with the PST-2 group well separated from pre-irradiation samples. (C) S-plot of important peak features derived from the o-PLSDA analysis. The most significant features ('rt_mz' ions) that distinguish the groups are represented in the bottom left and top right quadrants. (D) Pattern Hunter Analysis: 25 top peak features ('rt_mz' ions) matching time progression changes in abundance from pre- to post-irradiation Day Two. Pattern Settings: 1 < 2 < 3 < 4 (PRE < PST0 < PST1 < PST2). Pink: increased abundance, blue: decreased abundance with time.

Monte Carlo simulations in figure 3. The number of increased breath VOC scans reached nearly 800 following the second fraction on day two.

3.4. VOCs biomarkers discriminate between pre-irradiation versus post-irradiation groups and increase over time

Sample peak features ('rt_mz') were also subjected to supervised multivariate analysis by orthogonal partial least squares discriminant analysis (*o*-PLSA) for a binary comparison of pre-irradiation versus all post-irradiation samples (figure 5, panel A). The groups were well separated with non-overlapping distinct populations (colored circles represent the 95% confidence intervals). A multigroup sparse partial least squares discriminant analysis (s-PLSDA) indicated overlapping populations between the post-irradiation day 0 and day 1 samples, while day 2 samples were more clearly distinguished. All three sampling days were distinct from the pre-irradiation samples (figure 5, panel B). Candidate biomarkers of radiation exposure were identified from a S-plot of the binary *o*-PLSDA. The strongest associated markers are located in quadrants at the top right (positively correlated with radiation exposure) and bottom left (negatively correlated with radiation

exposure) (figure 5, panel C). Selected biomarkers are also shown in table 1.

Features were also analyzed using the Pattern Hunter tool in MetaboAnalyst to identify specific features that were positively correlated in abundance over time between pre-irradiation and post-irradiation day 0,1 or 2 samples (pattern $1 < 2 < 3 < 4$), as well as those that were negatively correlated (pattern $1 > 2 > 3 > 4$). The top 25 overall features are shown in figure 5, panel 5. The unidentified VOC#1 was the top feature that was associated with a dose/time dependent increase.

3.5. Structural identification of the most significant biomarker VOCs

Table 1 displays the most accurate VOC biomarkers of radiation exposure as shown by their C-statistic values. Alkane and alkane derivatives in the table included 2,2,4-trimethylhexane, 2,4-dimethylhexane, hexane, and 3-methylpentane; these VOCs were consistent with oxidative stress products of polyunsaturated fatty acids. An unidentified component (VOC#1) was the most accurate biomarker of radiation: its mass spectrum resembled 1H-Indene, octahdyro-2,2,4,4,7,7,-hexamethyl-, trans-, but its comparatively low R match value 695 did not permit structural identification. There was a linear relationship between the abundance of this VOC and the cumulative dose of radiation (figure 6).

4. Discussion

The main finding of this study was that TBI of non-human primates elicited a prompt and statistically significant increase in the abundance of a broad range of VOCs in the breath. Many VOC features were increased more than five-fold, increased over time and were sensitive and specific for radiation exposure during all three days of the study. Straight-chain n-alkanes and methylated alkanes were prominent among the VOCs that were most increased, consistent with metabolic products of oxidative stress (table 1).

The unidentified VOC#1 was the most accurate biomarker of radiation: it increased linearly and more than ten-fold with the total cumulative dose of radiation (figure 6). The source and identity of VOC#1 is not known, though a breath VOC with a similar spectrum has been reported in patients with lung cancer [19]. Indene can be formed from the reaction of benzene with allyl radicals [20], and both are metabolic products of radiation [10, 12, 21, 22].

We considered two main sources of potential error in this study: 'voodoo correlations' and misidentification of the chemical structure of biomarker VOCs.

The problem of 'voodoo correlations' was first employed in the neurosciences and it is now recognized as a common source of error in the analysis of large data sets. It describes a statistically significant correlation between two or more variables that was actually a random event [23, 24]. The problem arises in 'big data' when a large number of variables are measured in a comparatively small number of subjects, thereby increasing the likelihood that chance alone incorrectly identifies apparently significant correlations. However, Monte Carlo simulations provide a valuable tool for excluding voodoo correlations with a candidate biomarker by comparing its C-statistic employing the correct diagnosis (disease or no disease) to its mean C-statistic value obtained when a random diagnosis is assigned several times. In this study, we employed Monte Carlo simulations to stratify several hundred candidate biomarkers in order to minimize the risk of chance associations and to identify the breath VOCs that were the most significant biomarkers of radiation exposure. We have previously reported similar applications of Monte Carlo simulations to exclude voodoo correlations in breath VOC biomarkers of other conditions including influenza vaccination [14], breast cancer [15], and pulmonary tuberculosis [16].

A second problem is the misidentification of unknown metabolite biomarkers through spectral database matching when complete spectral deconvolution is not possible or the database is incomplete. A component's GC EI-MS spectrum provides a reproducible fingerprint of its fragmentation pattern that can be matched for similarity to large MS spectral database libraries, e.g. NIST GC-MS Spectral library. However, high probabilities for correct identifications are contingent on clean deconvoluted spectra and the inclusion of the compounds in the database. Even though GC-MS is a well-established technology, it can potentially misidentify an unknown VOC in a complex mixture like human breath which may contain hundreds or even thousands of components at trace levels [25]. We observed many overlapping component peaks in the chromatograms that could not be adequately deconvoluted especially in the central crowded region between RT = 8–13 min. Consequently, minor fragment peaks from co-eluting components likely contributed to somewhat lower R Match values. An R Match score greater than 800 generally indicates a good spectral match. A number of components listed in table 1 were tentatively identified based on their spectral similarity and high R Match values to hydrocarbon metabolites present in the NIST 2017 spectral library. Others such as VOC # 1 (RT = 12.83 min) suggest similarity to compounds with more complex hydrocarbon backbone structures but were not definitively identified. Rigorous confirmation of structural identity requires analysis of a sample of the pure compound and comparison of its RT and mass spectrum to those of the VOC observed in breath, which was beyond the scope of this study.

Table 1. Structural identification of the most significant biomarker VOCs. Candidate breath VOC biomarkers of radiation were identified with multiple Monte Carlo simulation (figure 3) and pattern recognition analysis (PLSDA and Pattern Hunter, figure 5). The table displays the main biomarker VOC peaks ranked according to their accuracy for detection of radiation exposure according to their *AUC* i.e. AUC of ROC curve (the C-statistic). RT is the retention time of the VOC in the chromatograph, *Identification* indicates the top compound match of the spectrum searched against the NIST 2017 database library of mass spectra and its associated CAS Registry Number. *R Match* indicates the probability scoring metric from the NIST database. A perfect match between a VOC spectrum and a library spectrum would result in an R Match value of 999; values above 800 indicate a good to excellent match. The VOC with the highest AUC (0.92) was designated as unidentified VOC#1 in view of its comparatively low R Match value.

AUC	RT (min)	Highest similarity in the NIST spectral database	CAS	R Match
0.92	12.83	1H-Indene, octahdyro-2,2,4,4,7,7,-hexamethyl-, trans- (IOH)	54832-83-6	695
0.88	2.48	Hexane	110-54-3	909
0.83	8.11	2,4-dimethylhexane	589-43-5	761
0.78	9.26	2,2,4-trimethylhexane	16747-26-5	696
0.77	5.73	Bicyclo[3.2.0]hepta-2,6-diene	2422-86-8	900
0.77	2.36	3-methlypentane	96-14-0	841
0.76	3.27	Acetic acid, hydrazide	1068-57-1	684

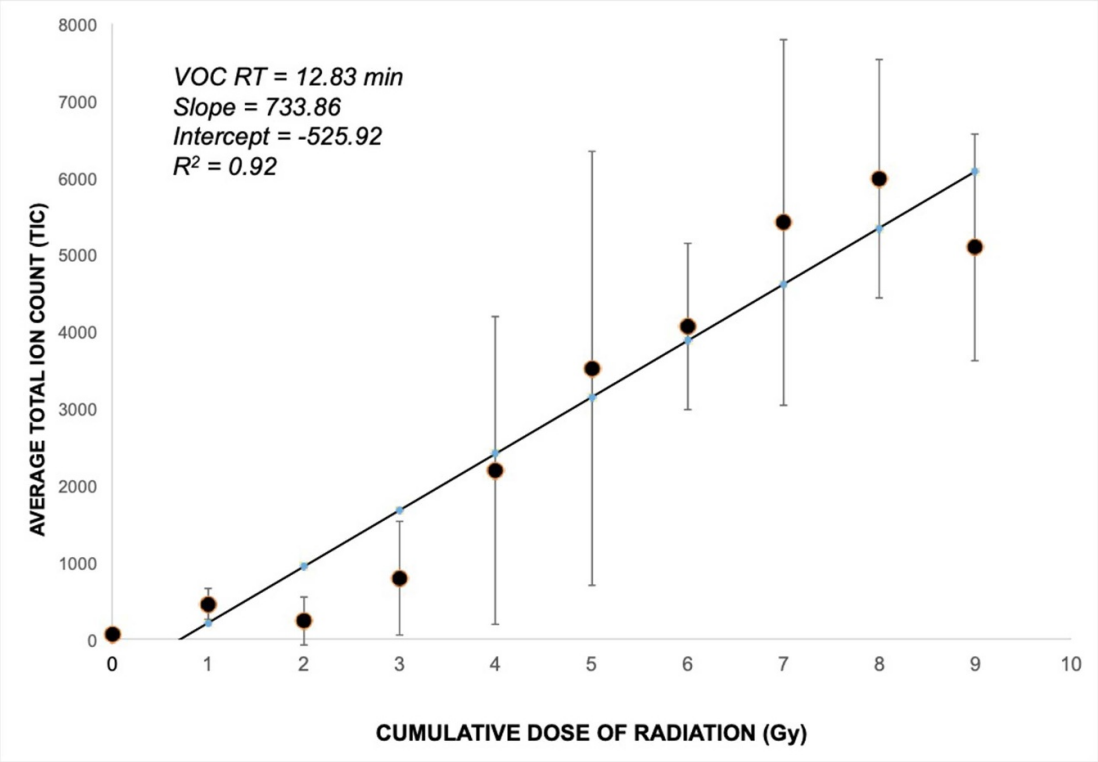

Figure 6. Dose-effect of unidentified VOC #1 versus cumulative dose of radiation. Monte Carlo simulations and MetaboAnalyst both ranked unidentified VOC #1 as the most significant candidate breath VOC biomarker of radiation exposure. The abundance of unidentified VOC #1, as shown by its average total ion count (TIC), varied linearly with the cumulative dose of radiation. Vertical lines display standard deviations of the TIC.

We also considered how the results might have been affected by potential confounding factors. For example, the increase in some biomarker VOCs may have been due to either continued exposure to radiation, or to the sustained effect of prior exposures before. Additional experimental studies would be required to address this point. Also, figure 2 demonstrates that some breath VOCs appeared to be reduced following radiation. This may have resulted from radiation-induced inhibition of upstream metabolic pathways or depletion of metabolites associated with oxidative stress protection, but further studies are required to explain this observation.

We conclude that TBI of non-human primates elicited a prompt and statistically significant increase in the abundance of several hundred VOCs in the breath. Many of these VOCs appeared to be sensitive and specific biomarkers of radiation exposure. These findings justify further evaluation of breath VOC biomarkers for use in radiation biodosimetry in humans.

Data availability statement

All data that support the findings of this study are included within the article (and any supplementary files).

Acknowledgments

Michael Phillips is President and CEO of Menssana Research, Inc. This project was funded by National Cancer Institute Contract No. 75N91019C00052

ORCID iD

Michael Phillips https://orcid.org/0000-0002-9889-131X

References

[1] Agrawala P K, Adhikari J S and Chaudhury N K 2010 Lymphocyte chromosomal aberration assay in radiation biodosimetry *J. Pharm. Bioallied Sci.* **2** 197–201
[2] Rana S *et al* 2010 Electron paramagnetic resonance spectroscopy in radiation research: current status and perspectives *J. Pharm. Bioallied Sci.* **2** 80–87
[3] Mitchell C R, Azizova T V, Hande M P, Burak L E, Tsakok J M, Khokhryakov V F, Geard C R and Brenner D J 2004 Stable intrachromosomal biomarkers of past exposure to densely ionizing radiation in several chromosomes of exposed individuals *Radiat. Res.* **162** 257–63
[4] Tucker J D, Grever W E, Joiner M C, Konski A A, Thomas R A, Smolinski J M, Divine G W and Auner G W 2012 Gene expression-based detection of radiation exposure in mice after treatment with granulocyte colony-stimulating factor and lipopolysaccharide *Radiat. Res.* **177** 209–19
[5] Marchetti F, Coleman M, Jones I M and Wyrobek A J 2006 Candidate protein biodosimeters of human exposure to ionizing radiation *Int. J. Radiat. Biol.* **82** 605–39
[6] Kneepkens C M, Ferreira C, Lepage G and Roy C C 1992 The hydrocarbon breath test in the study of lipid peroxidation: principles and practice *Clin. Invest. Med.* **15** 163–86
[7] Kneepkens C M, Lepage G and Roy C C 1994 The potential of the hydrocarbon breath test as a measure of lipid peroxidation *Free Radic. Biol. Med.* **17** 127–60
[8] Arterbery V E, Pryor W A, Jiang L, Sehnert S S, Michael Foster W, Abrams R A, Williams J R, Wharam M D and Risby T H 1994 Breath ethane generation during clinical total body irradiation as a marker of oxygen-free-radical-mediated lipid peroxidation: a case study *Free Radic. Biol. Med.* **17** 569–76
[9] Barba C, Santa-Maria G, Herraiz M and Calvo M M 2012 Rapid detection of radiation-induced hydrocarbons in cooked ham *Meat Sci.* **90** 697–700
[10] Zhu M J, Mendonca A, Lee E J and Ahn D U 2004 Influence of irradiation and storage on the quality of ready-to-eat turkey breast rolls *Poult. Sci.* **83** 1462–6
[11] Ismail H A, Lee E J, Ko K Y and Ahn D U 2009 Fat content influences the color, lipid oxidation, and volatiles of irradiated ground beef *J. Food Sci.* **74** C432–40
[12] Phillips M *et al* 2013 Detection of volatile biomarkers of therapeutic radiation in breath *J. Breath Res.* **7** 036002
[13] Phillips M, Cataneo R N, Chaturvedi A, Kaplan P D, Libardoni M, Mundada M, Patel U, Thrall K D and Zhang X 2015 Breath biomarkers of whole-body gamma irradiation in the Gottingen minipig *Health Phys.* **108** 538–46
[14] Phillips M, Cataneo R, Chaturvedi A, Danaher P J, Devadiga A, Legendre D A, Nail K L, Schmitt P and Wai J 2010 Effect of influenza vaccination on oxidative stress products in breath *J. Breath Res.* **4** 026001
[15] Phillips M, Cataneo R N, Saunders C, Hope P, Schmitt P and Wai J 2010 Volatile biomarkers in the breath of women with breast cancer *J. Breath Res.* **4** 026003
[16] Phillips M, Basa-Dalay V, Bothamley G, Cataneo R N, Lam P K, Natividad M P R, Schmitt P and Wai J 2010 Breath biomarkers of active pulmonary tuberculosis *Tuberculosis* **90** 145–51
[17] Cook N R 2008 Statistical evaluation of prognostic versus diagnostic models: beyond the ROC curve *Clin. Chem.* **54** 17–23
[18] Chong J and Xia J 2020 Using MetaboAnalyst 4.0 for metabolomics data analysis, interpretation, and integration with other omics data *Methods Mol. Biol.* **2104** 337–60
[19] Saidi T M *et al* 2020 Non-invasive prediction of lung cancer histological types through exhaled breath analysis by UV-irradiated electronic nose and GC/QTOF/MS *Sens. Actuators* B **311** 127932
[20] McCabe M N, Hemberger P, Reusch E, Bodi A and Bouwman J 2020 Off the beaten path: almost clean formation of indene from the ortho-benzyne + allyl reaction *J. Phys. Chem. Lett.* **11** 2859–63
[21] Baine T J and Sagstuen E 1998 Radiation-induced radical formation in beta-glycerophosphate single crystals studied by electron paramagnetic resonance and electron nuclear double resonance spectroscopy: formation of an allylic-type radical *Radiat. Res.* **150** 148–58
[22] De Cooman H, Pauwels E, Vrielinck H, Sagstuen E, Van Doorslaer S, Callens F and Waroquier M 2009 ENDOR and HYSCORE analysis and DFT-assisted identification of the third major stable radical in sucrose single crystals X-irradiated at room temperature *Phys. Chem. Chem. Phys.* **11** 1105–14
[23] Fiedler K 2011 Voodoo correlations are everywhere-not only in neuroscience *Perspect. Psychol. Sci.* **6** 163–71
[24] Rosenblatt J D and Benjamini Y 2014 Selective correlations; not voodoo *Neuroimage* **103** 401–10
[25] Phillips M, Cataneo R N, Chaturvedi A, Kaplan P D, Libardoni M, Mundada M, Patel U and Zhang X 2013 Detection of an extended human volatome with comprehensive two-dimensional gas chromatography time-of-flight mass spectrometry *PLoS One* **8** e75274